Sixth International Symposium on Turbulence and Shear Flow Phenomena
Seoul, Korea, 22-24 June 2009

DRAG FLUCTUATIONS ON DEFORMED BUBBLES IN A TURBULENT SHEAR FLOW BY MEANS OF DNS

Yoshinobu Yamamoto
Department of Nuclear Engineering,
Kyoto University
Yoshida, Sakyo, Kyoto 606-8501, Japan
yyama@nucleng.kyoto-u.ac.jp

Tomoaki Kunugi
Department of Nuclear Engineering,
Kyoto University
Yoshida, Sakyo, Kyoto 606-8501, Japan
kunugi@nucleng.kyoto-u.ac.jp

Kazuyuki Takase
Japan Atomic Energy Agency
Tokai, Naka, Ibaraki 319-1195, Japan
kazuyuki.takase@jaea.go.jp

ABSTRACT

In this study, the direct numerical simulation of a fully-developed turbulent channel flow with deformed bubbles were conducted by means of the MARS method, turbulent Reynolds number 150, and Particle Reynolds number 120. As the results, large scale wake motions round bubbles were confirmed. At the bubble related region, mean velocity was degreased and turbulent intensites and Reynolds shear stress were incresed by the effects of the large scale wake motions round bubbles. On the other hands, near wall region, effects of bubbly flow might act on flow laminarlize and drag reduction.

Two types of drag coefficient of bubble were estimated from the accelerated velocity of bubble and experimental equation as a function of Particle Reynolds number. Drag coefficient estimated by the accelerated velocity of bubble was below the results estimated by the experimental equation.

INTRODUCTION

Turbulent flows with bubbles are very often found in engineering devices such as a light-water nuclear reactor and chemical reactor. Therefore, both experimental and numerical investigations have been conducted, extensively. In the view points of understanding coherent structures and turbulent statistics behaviours, the DNS (Direct Numerical Simulation) is expected to have advantages of the experimental approaches. Recently, DNS of the turbulent shear flows with deformability bubbles have been conducted by Kawamura and Kodama, 2002, Lu et. al., 2005 and Lu and Tryggvason, 2008, based on the front-tracking method. These DNS focused on interaction between turbulent structures near wall and bubbles to investigate friction drag reduction effects on wall.

In this study, DNS of a fully-developed turbulent channel flow with bubbles were conducted to investigate forces acted on deformability bubbles such as drag coefficient.

NUMERICAL METHOD

Numerical procedure was based on the MARS method (Kunugi, 1997, Kunugi, 2001); the governing equations are consisted of Navier-Stokes equations with the CSF (Continuum Surface Force) model (Brackbill, 1992) , continuity equation and transport equations of a volume fraction function (VOF) F. To refine the suface tention acted on bubbles, a kind of a level-set function estimated by using VOF function, was used for calculation of the surface tention. As for the discretization of the governing equations on the Cartesian coordinate system, the second-order scheme for the spatial differencing terms is used on the staggered grid system. Time integration method was low-storage 3rd-order Runge-Kutta scheme for convection terms, Crank-Nicolson scheme for viscous terms and Euler Implicit scheme for Pressure terms, respectively. The physical problem treated here is the motion of two Newtonian incompressible fluids allowed the interface deformation between them.

NUMERICAL CONDITION

Figure 1 shows flow geometry and coordinate systems and Numerical condition was tabled in Table 1. In this study, minimum flow units (Jimenez and Moin, 1991) was selected as numerical domain. Thermal properties at normal air-water system were adapted. A fully developed single-phase turbulent channel flow data was used as the initial velocity fields and 4 bubbles which diameter was 1 mm were entrained in channel center domain.

Tabel 1 Numerical condtion

CASE	Re_τ	r^+	ρ_w/ρ_g	Domain $Lx\times Ly\times Lz$	Grid number $Nx\times Ny\times Nz$	Resolution $\Delta x^+,\Delta y^+,\Delta z^+$	T_0^+
CASE1	150	30	842.1	$4h\times 2h\times 4/3h$	150×134× 50	4.0, 0.5-4.0,4.0	420
CASE2	150	30	842.1	$4h\times 2h\times 4/3h$	300×182×100	2.0, 0.5-2.0,2.0	400

$Re_\tau = u_\tau h/\nu_w$: Turbulent Reynolds number, u_τ: Friction velocity at wall, $2h$: water depth,
ν_w: Kinetic viscosity of water, r: Initial radius of bubbles, ρ_w : Density of water, ρ_g :Density of air,
Lx, Ly, Lz: Computational domain, Nx, Ny, Nz: Grid number,
$\Delta x^+,\Delta y^+,\Delta z^+$: Grid resolution for stream (x)-, vertical (y)-, and span (z)- wise directions, respectively.
Super-script + denotes the nondimensional quantities normalized by friction velocity and kinetic viscosity used Reynolds number definition. T_0^+: Time integration length from initial condition to fully-developed status

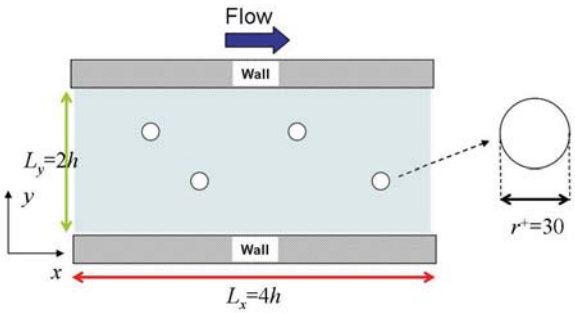

Fig.1 Flow geometry and coordinate system

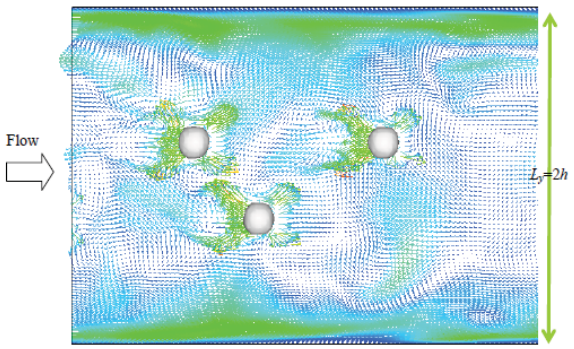

Fig.2-(a) Instantaneous turbulent velocity vector plots, side view, CASE1

Table 2 Numerical results

CASE	Re_p	r/r^+	Void fraction
CASE1	122	1.07	0.15%
CASE2	132	1.12	0.15%

$Re_p = |u_w - u_b|r/\nu_w$: Particle Reynolds number,
u_w: velocity of water, u_w: velocity of bubble,
ν_w: Kinetic viscosity of water,
r: Initial radius of bubbles, r'^+: Maximum radius of bubbles

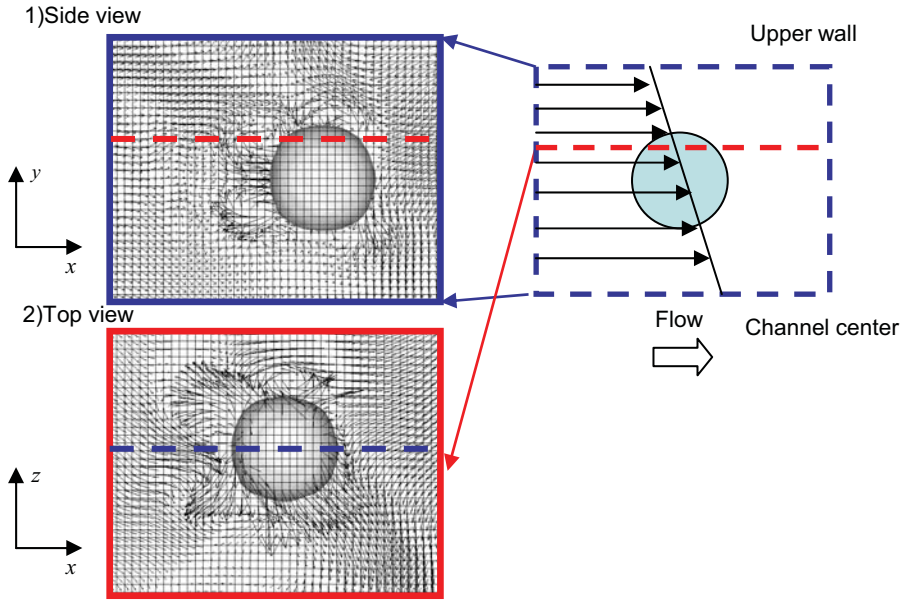

Fig.2-(b) Instantaneous turbulent velocity vector plots, side view and top view, CASE2

To obtain a fully-developed status, gravity effect was ignored and streamwise constant pressure gradient was forced on water phase. Non-slip at the walls and periodic conditions for stream and spanwise directions were adapted for boundary conditions.

The first time integration was conducted during 400 non-dimensional times ($T_0^+ = T_0 u_\tau^2/\nu$) from initial condition and Particle Reynolds number was kept in the equilibrium status. Secondary, 1200 non-dimensional time integration was conducted after fully-developed status to obtain statistics data.

EFFECTS OF GRID RESOLUTION

Figure 2-(a) and (b) show instantaneous turbulent velocity vector plots round bubbles after fully-developed status in CASE1 (Fig.2-(a)) and CASE2 (Fig.2-(b)), respectively. Large scale wake motions from the effect of bubbles on were confirmed. These motions round bubbles were no much difference between CASE1 and CASE2. Averaged particle Reynolds number and maximum longest diameter in both cases were tabled in Table 2. Both of Particle Reynolds number and longest diameter in CASE2 exceeded the results in CASE1 but these differences were slight.

MEAN AND STATISTICS

Figure 3 shows mean volume-rate function distribution in CASE1. Due to the neglect gravity effects, bubble motion for vertical direction was small and fluctuations of vertical bubble positions were within 20 in wall-units.

Water-phase mean velocity profile was shown in Fig.4. Mean velocity at channel center region and mean discharge was decreased compared with single-phase flow. This indicates that bubbles works as flow drag in this flow condition. Figure 5 and 6 show water-phase turbulent intensity and Reynolds shear stress profiles, respectively. Near channel center, turbulent intensities and Reynolds shear stress were increased compared with in case of single-phase flow. This is because form large scale wake motions as shown in Fig.2. On the other hands, in case of bubbly flow, peak position of streamwise turbulent intensity was slightly shifted to channel center and Reynolds stress near wall was decreased compared with single-phase flow case. Consequently, it seems that effects of bubbly flow act on flow laminarlize and drag reduction.

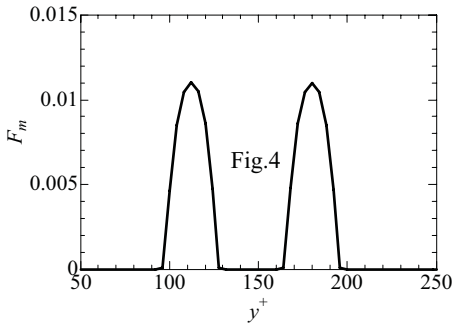

Fig.3 Distribution of mean volume-rate function

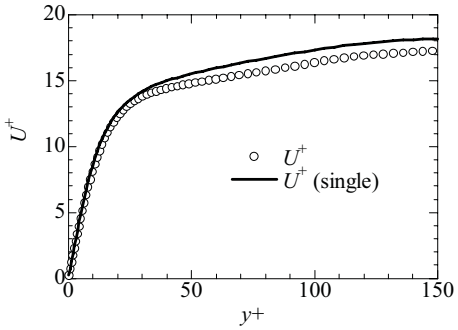

Fig.4 Mean velocity profiles

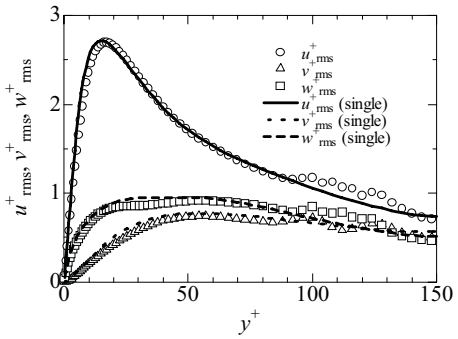

Fig.5 Turbulent intensity profiles

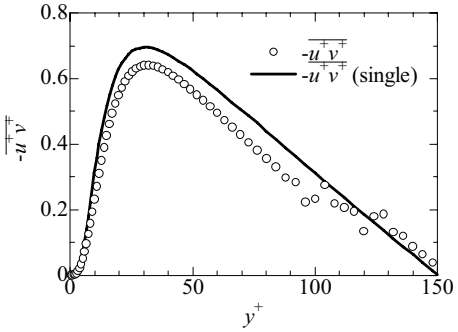

Fig.6 Reynolds shear stress profiles

PARTICLE REYNOLDS STRESS AND DRAG COEFFICENT

In this study, drag coefficient of bubbles was defined as follow,

$$\frac{d^2X}{dt^2} = F_D / m, \tag{1}$$

$$F_D = -\frac{C_D}{2}\rho_a \left(u_p - u_b\right)\left|u_p - u_b\right|\frac{\pi D^2}{4} \tag{2}$$

, where X is the position of bubble center, F_D is the forces acting on bubbles, m is the mass of bubble, C_D is the drag coefficient of bubble, u_p is the bubble velocity, u_b is the water-phase velocity and D is the initial bubble diameter,

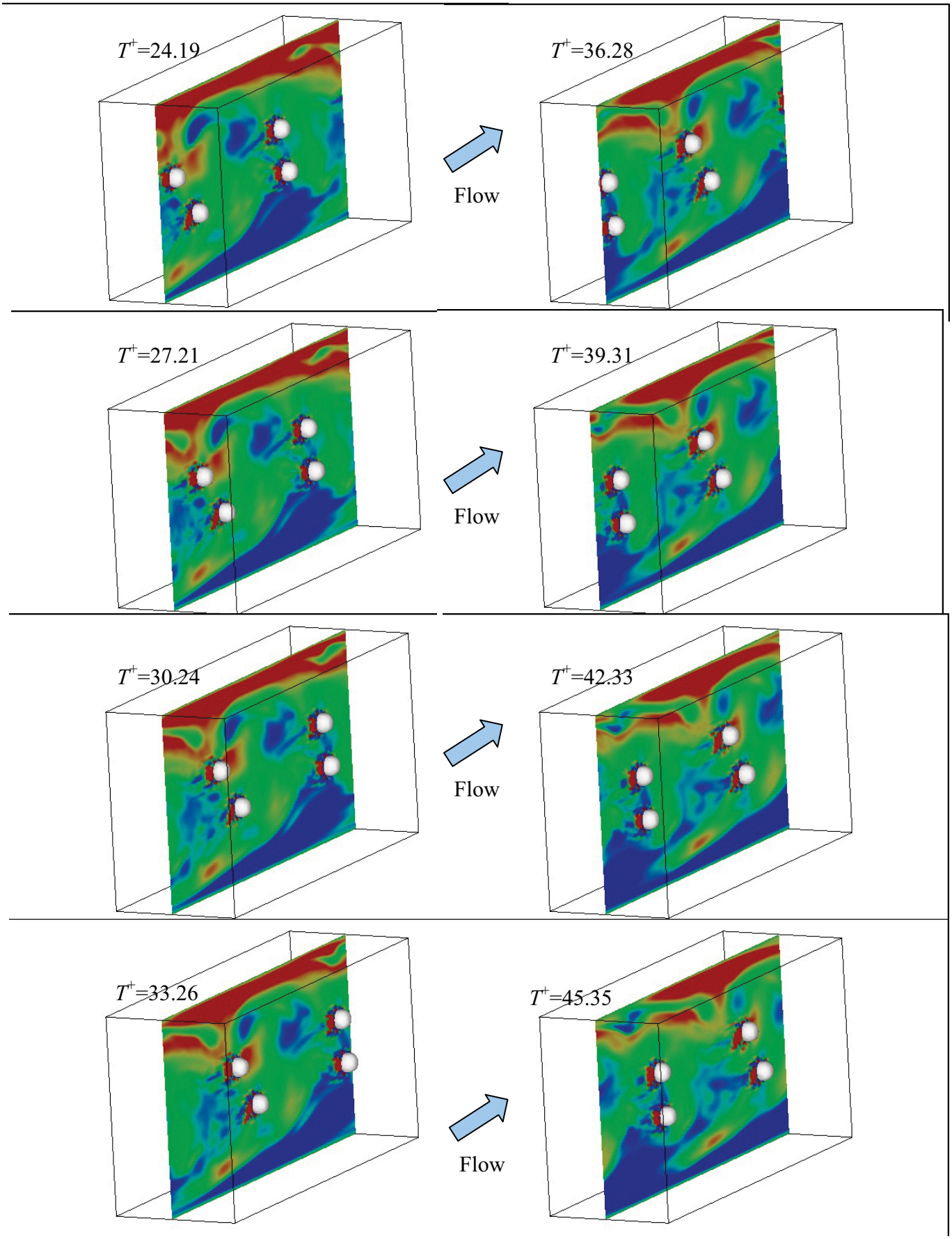

Fig.7 Instantaneous bubble behaviours with streamwise turbulent velocity contour plots
-3.5(Blue)<u^+<3.5(Red)

respectively. From equation (1) and (2), drag coefficient of bubble can be estimated as follow,

$$C_D = \frac{8Da}{6\left|u_p - u_b\right|^2} \tag{3}$$

, where $a(=d^2X/dt^2)$ is the accelerated velocity of bubble. In case of Particle Reynolds number was given and bubble deformation can be ignored, drag coefficient was also estimated by using experimental equation.

$$C_D = \left(0.55 + 4.8/\sqrt{Re_p}\right)^2, 1 < Re_p \le 1000$$
$$Re_p = \frac{\left|u_p - u_b\right| D}{\nu} \tag{4}$$

In this study, drag coefficient of bubble was estimated from equation (3) and (4), by using DNS data.

Figures 7 and 8 show instantaneous bubble behaviours with streamwise turbulent velocity contour plots and time series of instantaneous Particle Reynolds number, respectively. After fully-developed status, large wake motion round bubbles were constantly observed but bubble deformation was not so remarkable, maximum longest diameter was about 1.07 times of initial bubble diameter.

Particle Reynolds number changed the range form 110 to 135 and its range was within the assumption of equation (4).

Figures 9 show the instantaneous drag coefficient of bubble. Mean water-phase velocity at bubble center position and bulk water-phase velocity was used in Fig.9-(a) and (b), respectively. Drag coefficient of bubble by using local water-phase velocity exceeded it by using bulk water-phase velocity. This is why relative velocity is increased in case of local-position velocity than bulk velocity.

Drag coefficient estimated by the accelerated velocity of bubble was below the results estimated by the experimental equation (4) in spite of the definition of water-phase velocity. In case of using local water-phase velocity (Fig.9-(a), drag coefficient estimated by the accelerated velocity was closed to its estimated by the experimental equation (4) than in case of using bulk velocity (Fig.9-(b)). This is caused from large scale wale motions as shown in Fig.2.

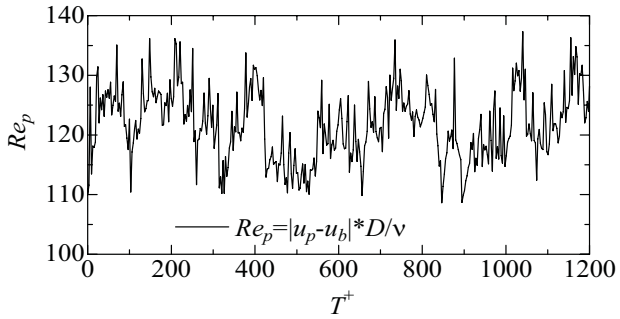

Fig.8 Time series of instantaneous Particle Reynolds number.

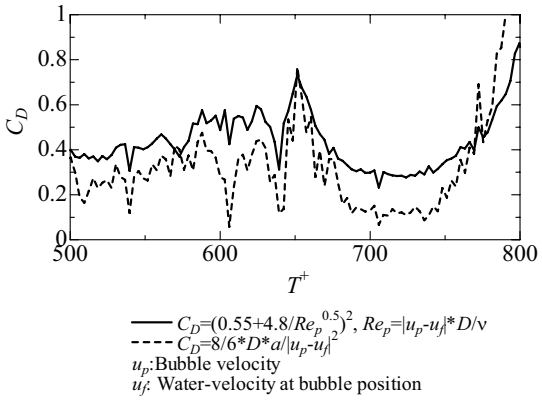

Fig. 9-(a) Drag coefficient of bubble
u_b: Mean water-phase velocity at bubble center position: u_f

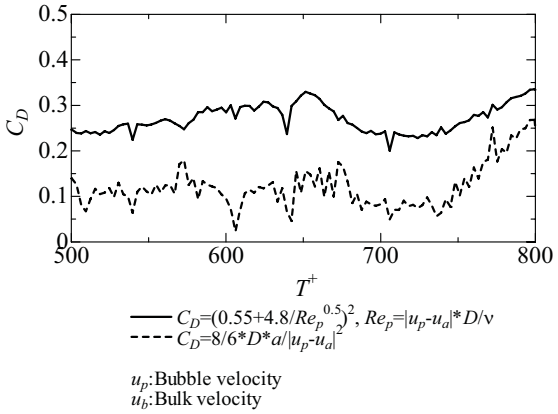

Fig. 9-(b) Drag coefficient of bubble
u_b: Bulk water-phase velocity

SUMMARY

In this study, the direct numerical simulation of a fully-developed turbulent channel flow with bubbles were conducted by means of the MARS method. DNS database such as the mean velocity, turbulent statistics and drag coefficent of deformed bubble were obtained. Main results are summarize as follow;

1) In this flow condition, average Particle Reynolds number about 120, large scale wake motions by the effect of bubbles were confirmed.
2) At the bubble related region, mean velocity was degreased and turbulent intensites and Reynolds shear stress were incresed by the effects of the large scale wake motions round bubbles.
3) Near wall region, peak position of streamwise turbulent intensity was slightly shifted to channel center and Reynolds stress near wall was decreased.
4) Drag coefficient estimated by the accelerated velocity of bubble was below the results estimated by the experimental equation.

ACKNOWLEDGEMENT

A part of the present study is the result of "Development of a high-precision numerical simulator based on the computer science approach for the evaluation of gas inclusion in FBR" entrusted to Nagoya Univ. by the Ministry of Education, Culture, Sports, Science and Technology of Japan (MEXT). And first author was also supported by Global COE program “Energy Science in the Age of Global Warming“, MEXT, japan.

REFERENCES

Brackbill, J.U. et al, J. Comput. Phys., 100(1992), pp.335-354.

Jimenez, J. and Moin, P., J. Fluid Mech., 225, 1991.

Lu, J. et. al., Physics of Fluids, 17, 2005. Lu, J. and G. Tryggvason, Physics of Fluids, 20, 2008

Kawamura, T. and Kodama, T., Int. J. Heat and Fluid Flow, 23, 2002.

Kunugi, T., Trans. JSME Ser. B, vol.63, no. 609(1997), pp.1576-1584.[in Japanese].

Kunugi, T., Comput. Fluid Dynamics J., vol.9, no.1 (2001), pp. 563-571.